NISTIR 7494

Effect of Artificial Perspiration and Cleaning Chemicals on Mechanical and Chemical Properties of Ballistic Fibers

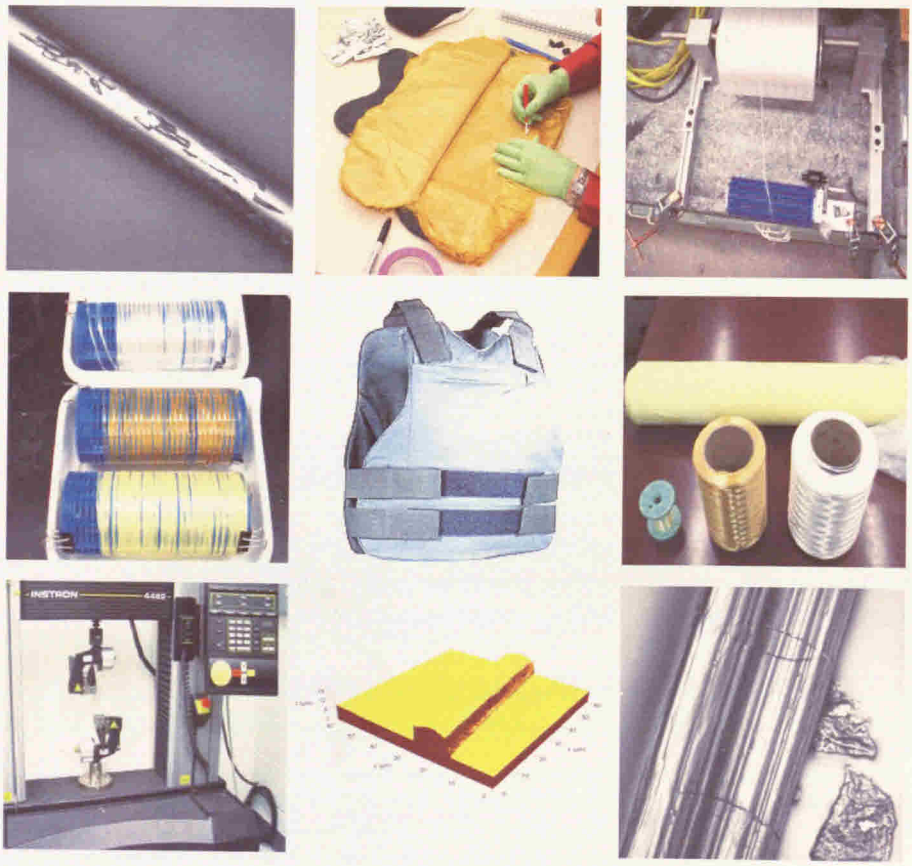

NIST
National Institute of Standards and Technology
Technology Administration, U.S. Department of Commerce

NISTIR 7494

Effect of Artificial Perspiration and Cleaning Chemicals on the Mechanical and Chemical Properties of Ballistic Fibers

Sylvain Petit and Joannie Chin
Polymeric Materials Group
Materials and Construction Research Division
Building and Fire Research Laboratory

Amanda Forster, Michael Riley and Kirk Rice
Office of Law Enforcement Standards
Electronics and Electrical Engineering Laboratory

Sponsored by:
National Institute of Justice
Office of Justice Programs
(Agreement number 2003IJR029)

June 2008

U.S. DEPARTMENT OF COMMERCE
Carlos M. Gutierrez, Secretary

NATIONAL INSTITUTE OF STANDARDS AND TECHNOLOGY
James M. Turner, Acting Director

Abstract

During routine field use of soft body armor, the ballistic panels often become saturated with perspiration. This condition motivates the user to clean and/or deodorize the armor, and anecdotal evidence is given for various methods used to accomplish this. While the cleaning/deodorization is usually performed on the armor liners and coverings, there is concern that the chemicals could seep into the ballistic panels. The purpose of this study is to assess the effect of perspiration and cleaning chemicals on the mechanical and chemical properties of aramid, poly(p-phenylene benzobisoxazole), and ultrahigh molecular weight polyethylene ballistic yarns and fabrics following controlled cycles of exposure to artificial perspiration and dilute solutions of common cleaning chemicals. It was observed that the effect of the artificial perspiration on properties of all materials tested was the same as that of water alone. Of all of the cleaning chemicals employed, only chlorine bleach had a detrimental effect on fiber properties that was above and beyond that of water alone. All other cleaning chemical solutions and artificial perspiration induced the same effects as water alone.

Key words: artificial perspiration, body armor, ballistic fibers, poly(benzazole), aramid, ultrahigh molecular weight polyethylene, chlorine bleach, infrared spectroscopy, confocal microscopy, tensile testing.

Introduction

During routine field use of soft body armor, the ballistic panels become saturated with perspiration. Although human perspiration is primarily composed of water, it also contains small quantities of organic compounds and inorganic salts. In the testing and qualification of body armor, questions have arisen as to whether plain water has an equivalent effect on the long term properties of ballistic fibers as does human perspiration.

In attempts to clean and deodorize body armor, anecdotal evidence exists that vest users spray the panels with odor neutralizer, disinfecting sprays, and cologne, as well as wipe them down with dilute solutions of detergent or bleach. Standard soft body armor is composed of multiple layers of ballistic fabric sealed into a woven fabric liner (referred to as the covering); this entire assembly is then inserted into a fabric carrier. Laundering of the ballistic panels and coverings is not recommended by body armor manufacturers. However, the carriers can be washed and dried using conventional home laundering techniques.

The purpose of this study is to assess the effect of artificial perspiration and dilute cleaning chemical solutions on the mechanical and chemical properties of poly(p-phenylene benzobisoxazole), poly(p-phenylene terephthalamide), and ultrahigh molecular weight polyethylene ballistic yarns and fabrics, using controlled cycles of exposure.

Overview of Fibers Studied

In this study, three main classes of commercial ballistic fibers used in body armor were studied: Poly(p-phenylene benzobisoxazole) (PBO), poly(p-phenylene terephthalamide), and ultrahigh molecular weight polyethylene (UHMWPE). The tensile properties of these fibers, as provided by their manufacturers, are shown in Table 1. An overview of each fiber type is provided below.

Poly(p-phenylene benzobisoxazole) (PBO)

Poly(p-phenylene benzobisoxazole)(PBO) is a member of the benzazole polymer family, and is characterized by the heterocyclic benzobisoxazole group in its main chain structure, as shown in Figure 1. The conjugated benzobisoxazole and phenyl rings in the PBO repeat unit contribute to extended π-electron delocalization and molecular rigidity, which provides high thermal stability and outstanding mechanical properties to this class of rigid-rod polymers. The PBO manufacturing process [1] involves wet-spinning from a poly(phosphoric acid) (PPA) solution. After spinning, the fiber is coagulated in water to remove the PPA.

PBO fibers, like the majority of polybenzazole-based fibers, are extremely strong, tough and stiff, with tensile strengths and moduli superior to those of aramid or ultra-high molecular weight polyethylenes. As is the case with most rigid rod polymers, the compressive strength of PBO is relatively poor, being approximately 10 % to 15 % of its tensile strength [2].

Previous research on the chemical resistance of PBO has documented significant losses in tensile strength following immersion in water, hydrochloric acid, nitric acid, sulfuric acid, sodium chloride, and sodium hypochlorite [3]. In a study of temperature and moisture effects on PBO fibers [4], changes in chemical, morphological, and

mechanical properties were observed following exposure. It was concluded that that one of the primary degradation mechanisms in PBO fiber is initiated by moisture in the external environment and that moisture initially present in the fiber is not the primary initiator of degradation.

Poly(p-phenylene terephthalamide) (aramid)

The chemical structure of poly(p-phenylene terephthalamide), commonly referred to as "polyaramid" or "aramid", is shown in Figure 2. The structure of poly(p-phenylene terephthalamide) consists of relatively rigid molecules, which form planar sheet-like structures. This material derives its strength from its highly crystalline structure containing inter-molecular hydrogen bonds between the carbonyl groups and protons on neighboring polymer chains and the partial π stacking of the benzenoid aromatic structures between stacked strands.

Aramid fiber is produced by solution spinning, using a co-solvent with an ionic component (calcium chloride) to occupy the hydrogen bonds of the amide groups, and an organic solvent (N-methyl pyrrolinidone) to dissolve the aromatic polymer. The use of concentrated sulfuric acid in aramid production is required to keep the highly insoluble polymer in solution during synthesis and spinning [5].

Although aramid fiber has neither the highest tensile strength nor modulus among the high performance fibers, it offers a favorable balance of key properties such as high tensile properties, light weight, chemical resistance, and thermal and dimensional stability. As with PBO, aramid fibers have relatively low axial and transverse compression properties as well as shear properties, due to the anisotropic structure of the fibers. In general, aramid fibers are resistant to most organic solvents, but are susceptible to attack by strong bases or acids at elevated temperatures or high concentrations.

Aramid fibers are hydrolyzed under certain conditions, but at a negligible rate under ambient conditions (nominally 23 °C and 15 % RH) [5].

Ultra high molecular weight polyethylene (UHMWPE)

The chemical structure of ultra high molecular weight polyethylene (UHMWPE), also known as high modulus polyethylene (HMPE) or high performance polyethylene (HPPE), is shown in Figure 3. UHMWPE fiber is a thermoplastic material which is highly resistant to corrosive chemicals, with the exception of oxidizing acids. It has extremely low moisture absorption and low coefficient of friction, is self- lubricating, and highly resistant to abrasion (10 times more resistant than carbon steel).

UHMWPE fibers are produced by the gel-spinning process using a 1 mass % to 5 mass % solution of polyethylene in paraffin oil [6]. Extrusion of this solution through a conical die at high temperatures yields a paraffin oil-containing fiber. The paraffin oil is removed by extraction with n-hexane. After drying, the fiber is hot-drawn to its maximum obtainable draw ratio, resulting in a dramatic improvement in properties. It has been shown that the ultimate fiber properties also depend strongly on spinning speed, spinning temperature, stretching in the spinline [6], molecular weight/weight distribution, polymer concentration, solvent quality, and die geometry.

Despite the relatively weak van der Waal's forces between the chains, UHMWPE fiber derives substantial strength from the length of the individual polymer molecules and their high degree of alignment. The fiber can attain a parallel orientation greater than 95 % and a degree of crystallinity of up to 85 %. In contrast, rigid rod polymers such as aramid derive their strength from strong hydrogen bonding between relatively short molecules [2].

As shown in Figure 3, the simple, non-polar structure of the molecule also gives rise to surface and chemical properties that are rare in high-performance polymers. Since these fibers do not contain polar chemical groups (such as esters, amides, or hydroxyls) that are susceptible to chemical and/or hydrolytic attack, they are very resistant to water, moisture, most chemicals, UV radiation, and micro-organisms. In the heterocyclic polymers, the polar groups bond easily to water. Because olefins have no such groups, UHMWPE does not absorb water readily. However, it is not easily wetted due to low surface energy, which makes bonding it to other polymers difficult.

Experimental Approach *

Materials

The types, properties and sources of the commercially available ballistic materials used in this study are listed below:

- Virgin aramid yarn, 1500 denier +
- Plain weave scoured aramid fabric constructed from 1500 denier aramid warp and fill yarns, areal density = 332 g/m^2, no surface treatment.
- Plain weave water-repellent treated aramid fabric constructed from 1500 denier aramid warp and fill yarns, areal density = 332 g/m^2, treated with a water repellent finish.
- Virgin ultrahigh molecular weight polyethylene (UHMWPE) yarn, 1350 denier.
- Virgin poly(phenylene benzobisoxazole) (PBO) yarn, 498 denier.

* Certain commercial equipment, instruments, or materials are identified in this paper in order to specify the experimental procedure adequately. Such identification is not intended to imply recommendation or endorsement by NIST, nor is it intended to imply that the materials or equipment identified are necessarily the best available for this purpose

+ "Denier" is a measure of linear mass density used by the textile industry, and is defined as mass in grams per 9000 m.

Artificial Perspiration

The composition of human perspiration depends on age, ethnicity, metabolism, and level of activity; thus, it is difficult to define a "standard" formulation for artificial perspiration. Although human perspiration is composed of 99 % water by mass, it also contains sodium chloride (NaCl), potassium chloride (KCl), urea, ammonium chloride (NH_4Cl), lactic acid, and acetic acid. Table 2 compares the composition of natural perspiration [7, 8] to artificial perspiration solutions. For this study, the perspiration solution recipe in ISO 3160-2 [9] was selected. Neither the pH of the artificial perspiration solution nor the plain water control changed significantly after 59 immersion cycles, as shown in Table 3.

Cleaning Chemicals

Separate 5 mass % solutions in distilled water were prepared for a commercially available odor neutralizer (Febreze, Meadow and Rain scent), liquid detergent (Tide, Original Scent), and chlorine bleach were utilized. The primary ingredients in the odor neutralizer are listed as cyclodextrin (odor eliminator derived from corn), water, ethanol, fragrance, and unspecified quality control agents. The active ingredients in the liquid detergent are biodegradable surfactants (anionic and non-ionic), ethanol, monoethanolamine, sodium tetraborate and unspecified enzymes. Chlorine bleach is a 6 mass % sodium hypochlorite solution in water, and also contains some unspecified ingredients. Solution pHs before and after 59 immersion cycles are shown in Table 3, and are not observed to change significantly during the exposure period, with the exception of the odor neutralizer solution, which decreased from pH = 8.80 to pH = 5.90. The reason for this is unknown.

Perspiration and Cleaning Chemical Exposure Cycles

As shown in Figure 4, PBO, aramid and UMHWPE yarns were wound on plastic dye tubes (Precision Spools, Inc.) having a length of 170 mm and a diameter of 54 mm. Fibers were wound gently to minimize damage which could result in a loss of mechanical properties. Yarn ends were secured to the dye tubes using metal binder clips covered with plastic bags to prevent corrosion.

Yarn tubes and fabric samples were immersed into the artificial perspiration solution and cleaning chemical solutions using a cycle that was composed of 1 h of immersion at room temperature followed by (3 to 4) d in a 40 °C oven, as shown in Figure 5. All analyses were carried out during the 40 °C phase of the immersion cycle. Specimens underwent 59 immersion/drying cycles (approximately 9 months of total test time). Due to the rapid deterioration of all fibers exposed to bleach solution, only 29 immersion/drying cycles (approximately 4 months) were utilized. For baseline measurements, one set of each material undergoing exposure was also cycled in plain distilled water and one set was stored at 40 °C.

Tensile Testing

For tensile testing of yarns, the appropriate lengths of yarn needed were measured and cut from the main spool at each inspection. For the fabric samples, individual yarns were extracted from the fabric for testing. To obtain yarn mechanical properties, tensile testing of yarns was carried out in accordance with ASTM D2256-02, "Standard Test Method for Tensile Properties of Yarn by the Single-Strand Method" using an Instron Model 4482 test frame equipped with a 91 kg (200 lb) load cell and pneumatic yarn and cord grips (Instron model 2714-006). Jaw separation was 7.9 cm (3.1 in) and cross-head speed was 2.3 cm/min (0.9 in/min). Yarns were nominally 6.3 cm (16 in) long, and given

64 twists (4 twists/in) on a custom designed yarn twisting device. This level of twist was maintained on the yarns as they were inserted into the pneumatic yarn and chord grips. A minimum of ten replicates was tested to failure. The standard uncertainty of these measurements is typically ± 5 %. Following each set of tests, a 25 cm length of fiber was stored for potential future analyses.

Infrared Analysis

Infrared analysis was carried out using a Nicolet Nexus FTIR equipped with a mercury cadmium telluride (MCT) detector and a SensIR Durascope attenuated total reflectance (ATR) accessory. Consistent pressure on the yarns was applied using the force monitor on the Durascope. Dry air was used as the purge gas. FTIR spectra were recorded at three different locations on each yarn and were averaged over 128 scans. Spectral analysis, including spectral subtraction, was carried out using a custom software program developed in the Polymeric Materials Group at NIST to catalogue and analyze multiple spectra [11]. The spectra were baseline corrected and normalized using the aromatic C-H deformation peak at 848 cm^{-1} for PBO, the aliphatic C-H bend at 1472 cm^{-1} for UHMWPE and the aromatic deformation peak at 820 cm^{-1} for aramid. Spectral subtraction was carried out by subtracting the baseline (unexposed) spectra from the spectra of the exposed materials. Standard uncertainties associated with this measurement are ± 4 cm^{-1} in wavenumber and ± 1 % in absorbance.

Laser Scanning Confocal Microscopy

A Zeiss Model LSM510 reflection Laser scanning confocal microscope (LSCM) was employed to qualitatively characterize the fiber surface morphology. The incident laser wavelength was 543 nm. By moving the focal plane in the z-direction, a series of

single images (optical slices) can be stacked and digitally summed over the z-direction to obtain a 3-D image. The *z*-direction step size was 0.5 μm using objectives of 5x and 10x, and 0.1 μm using objectives of 20x, 50x, and 150x. At a magnification of 150x, the dimensions of each image are 61.4 μm by 61.4 μm (512 pixels by 512 pixels).

Results and Discussion

Tensile Properties

Tensile properties of ballistic fibers are critical to the ballistic performance of soft body armor [12]; hence, it is necessary to be cognizant of factors that can cause physical or chemical damage and subsequently degrade fiber tensile properties. The evolution of tensile strength, elongation at break and tensile modulus for aramid, UHMWPE and PBO are shown as a function of immersion cycles in Figures 6-10. Table 4 presents the percentage change in yarn tensile properties after 29 cycles of immersion in bleach solution and 59 cycles in water, odor neutralizer, and detergent solutions. The percentage change corresponds to:

$$[(\text{property}_{\text{final}} - \text{property}_{\text{initial}})/ \text{property}_{\text{initial}}] \times 100$$

To determine the statistical significance of observed changes in tensile properties relative to the baseline, a two population t-test [13] with a confidence interval of 95 % was carried out on the data.

Before discussing the tensile data, it must be noted that slippage of UHMWPE yarns periodically occured when using grips with 1.75 kN capacity. This was particularly problematic for UHMWPE fibers immersed in the detergent solution. In subsequent testing of UHMWPE, it was found that the use of 2.0 kN grips alleviated this problem.

In evaluating the effects of the exposure conditions on fiber properties, it must be noted that all immersion environments were aqueous in nature, so any observed effects would also include the contribution of water. Both the aramids and PBO are known to be susceptible to hydrolysis [14, 15], and exhibited decreases in tensile properties following water exposure in this study. Since UHMWPE is non-polar, no decreases in tensile properties following water exposure were observed. To determine the statistical significance of observed changes in tensile properties following artificial perspiration and cleaning chemical exposure relative to the changes in tensile properties following plain water exposure, a two population t-test with a confidence interval of 95 % was applied to the data.

It is puzzling why the fibers which were continuously stored at 40 °C during the study also exhibited changes in tensile properties. It is speculated that because all of the materials were stored in the same 40 °C oven, the local relative humidity in the oven was raised for a short period of time each time the wet specimens were replaced after the aqueous immersion portion of the cycle. This repeated, short-term exposure to elevated relative humidity may have contributed to the decreases in tensile properties observed for this set of materials. Thus, no conclusion could be drawn as to whether or not the 40 °C drying step contributed to any observed deterioration in tensile properties.

In general, the organic and inorganic compounds in the artificial perspiration solution, detergent or odor neutralizer did not appear to play a statistically significant role in additional fiber degradation beyond that of water, as determined by the two population t-test with a confidence interval of 95 %. The only exception was that of virgin aramid yarn, which exhibited decreases in tensile properties beyond that induced by water following exposure to artificial perspiration and odor neutralizer solutions.

After 29 bleach solution exposure cycles, all materials exhibited substantial decreases in tensile strength, elongation at break, and tensile modulus that were statistically different from changes produced by plain water, as determined by the t-test. Commercial chlorine bleach is essentially an aqueous solution of sodium hypochlorite, which is a strong oxidizer. In water, sodium hypochlorite hydrolyses into sodium hydroxide and hypochlorous acid. Both compounds are known to contribute to hydrolysis of PBO and aramid-based materials [3, 5].

Relative to the baseline values, decreases in tensile strength following bleach solution exposure were 19 % for UHMWPE, between 50 % and 60 % for the various aramids, and 45 % for PBO. Elongation at break following bleach exposure was unchanged for UHMWPE, but decreases in elongation at break were observed for both the aramids (33 % - 49 %) and PBO (40 %). Changes in tensile modulus induced by bleach solution were minimal for UHMWPE, but were substantial for the aramids (15 % - 29 %) and PBO (10 %). In reference [3], a 48 % loss in tensile strength of PBO was reported after a 100 d exposure to hypochlorite bleach solution.

A comparison of the yarns extracted from the scoured and water repellent-treated fabrics to the virgin aramid yarn revealed that, with the exception of the bleach exposures, the water repellent-treated fabric exhibited a smaller degree of loss in properties than its scoured counterpart. It is speculated that the water repellent treatment on the fiber was compromised by the bleach solution, but it did serve to partially protect the fabric from the effect of the various solutions.

It is also hypothesized that in a woven fabric, properties of the individual yarns are affected by the weaving operation and are in turn affected more by their external environment. Yarns in a carefully woven aramid fabric may retain 90 % to 95 % of their original tensile strength, while in a poorly woven fabric, individual yarns may be

damaged and retain only 80 % to 90 % of their original tensile strength. Yarn finishes and sizing also impact the extent of damage incurred by yarns during weaving and thus tensile strength retention [5]. However, there were no clear trends observed in the behavior of the yarns extracted from the aramid fabrics compared to the aramid yarn.

Surface Morphology

Confocal microscopy was carried out to visually and qualitatively assess changes in the fiber surface morphology. Representative confocal images showing fibers prior to immersion, after 29 cycles of water immersion, and after 29 cycles of bleach solution immersion are shown in Figures 11 – 15. After 29 cycles of bleach immersion, significant pitting was observed on all fiber surfaces. The surface morphology of the water-exposed aramids and UMHWPE, (shown in Figures 11-13 and Figure 14, respectively) was unchanged relative to the unexposed specimens. This indicates that the surface morphology changes observed in the bleach-exposed fibers are due to the oxidizers in the bleach solution, and not to water exposure. In the PBO confocal micrographs shown in Figure 15, differences in surface morphology are observed between the unexposed fibers and both the water-exposed and bleach exposed fibers. Very little difference in surface appearance is observed between the water-exposed fibers and the bleach-exposed fibers. However, since the tensile properties of the bleach-exposed yarns were more highly degraded than those of the water-exposed yarns, it is speculated that the damage initiated by the bleach exposure penetrated deeper into the bulk of the fiber

Chemical Structure

Changes in the intensities or frequencies of observed infrared spectral peaks can be correlated to changes in the molecular structure of the compound. Spectral subtraction, in which a reference spectrum is subtracted from the spectrum of a material of interest, is helpful in extracting small chemical changes and providing information on the formation and depletion of specific functional groups. In addition to the references given, peak assignments are made with the guidance of reference [16].

In the difference spectra presented in this section, downward-pointing, or negative, peaks are species that are lower in concentration relative to the reference spectrum (unexposed materials, in this case), and upward-pointing, or positive, peaks are species that are higher in concentration relative to the reference material or new species that are not originally present in the reference material. In the interest of space, spectra are only shown here for specimens following bleach solution immersion.

The infrared spectrum of aramid yarn and resulting difference spectrum after bleach exposure is shown in Figures 16(a) and 16(b). Results for the scoured and water-repellent treated aramid fabrics are very similar and are not shown here. As shown in Figure 16(a), characteristic infrared peaks for aramids are the amide N-H stretching at 3320 cm^{-1}, carbonyl stretching at 1640 cm^{-1} (amide I), N-H bending/C-N stretching interactions at 1535 cm^{-1} and 1513 cm^{-1} (amide II), and C-N stretching at 1305 cm^{-1} [17]. The difference spectrum in Figure 16(b) shows new broad peaks centered at 3400 cm^{-1} and 3200 cm^{-1}, which are attributed to a combination of amine N-H stretching, and carboxylic acid OH stretching. New peaks are also observed at 1570 cm^{-1} and 1420 cm^{-1} that attributed to carboxylate ion stretching. Negative peaks with positions corresponding to the original amide I, amide II, and C-N stretching peaks are also observed. This

evidence points to the hydrolysis of the main chain amide group to amine and carboxylic acid [14]:

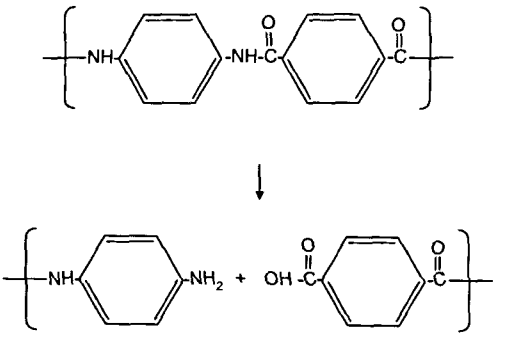

This degradation mode results in chain scission and subsequent loss of tensile properties.

The spectrum of UMHWPE and the resulting difference spectrum following bleach exposure are shown in Figures 17(a) and 17 (b). Figure 17(a) shows the characteristic peaks for UMHWPE, identified as C-H stretching at 2914 cm^{-1} and 2846 cm^{-1}, and C-H bending at 1470 cm^{-1} and 1461 cm^{-1}. The difference spectrum in Figure 17(b) shows new peaks at 3400 cm^{-1} (broad), attributed to O-H stretching from an oxidized species, and 1573 cm^{-1} and 1420 cm^{-1}, characteristic of carboxylate ion stretching. Negative peaks corresponding to the original C-H stretching peaks at 2914 cm^{-1} and 2846 cm^{-1} are also observed, indicating a change in the original polyethylene structure. Similar changes in chemical structure have been observed for polyethylene exposed to oxidizing conditions, which cause chain scission or crosslinking of the polyethylene chains, and leads to degradation of polyethylene mechanical properties [18,19].

In the spectrum of PBO shown in Figure 18(a), peaks at 1620 cm^{-1}, 1056 cm^{-1}, 925 cm^{-1}, and 914 cm^{-1} are identified as stretching modes associated with the benzoxazole ring, which is the most prominent chemical feature of PBO [20]. Following bleach exposure, the difference spectrum in Figure 18(b) reveals a broad new peak centered at

3400 cm^{-1}, which is a complex combination of amine N-H stretching, and O-H stretching from carboxylic acids or phenols, and peaks at 1589 cm^{-1}, 1423 cm^{-1}, and 1369 cm^{-1}, which are collectively attributed to carboxylate ion stretching, and/or carboxylic acid C-O stretching and O-H bending. Negative peaks are found at 1056 cm^{-1} and 925 cm^{-1}, which are the peak positions associated with the benzoxazole ring. This evidence provides support for a degradation mechanism that involves hydrolysis of the benzoxazole ring to benzamide

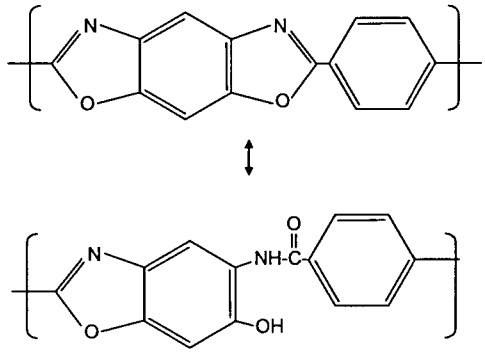

and subsequently to aminophenol and carboxylic acid:

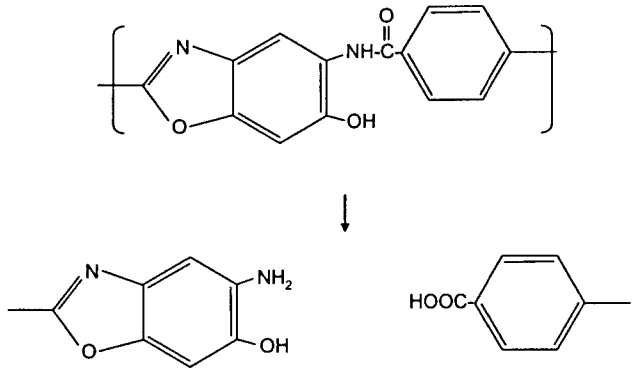

Similar observations have been made by other researchers in the study of PBO hydrolysis [15, 21].

Summary and Conclusions

The effects of perspiration and cleaning chemicals (odor neutralizer, solution, liquid detergent solution, and chlorine bleach) on the tensile, chemical and surface morphological properties of aramid yarns and fabrics, UHMWPE yarn, and PBO yarn were investigated using controlled immersion/drying cycles.

The tensile properties of aramid and PBO materials decreased following exposure to plain water, artificial perspiration, and 5 mass % solutions of detergent, odor neutralizer, and chlorine bleach. The hydrophobic UHMWPE exhibited tensile strength decreases only in chlorine bleach. For all materials tested, only chlorine bleach caused a significant decrease in tensile properties *beyond* that of plain water. No degradation of tensile properties beyond that induced by plain water was observed following artificial perspiration exposure for any of the ballistic materials.

Analysis of fiber surface morphology after exposures revealed that chlorine bleach caused physical changes in the fiber surfaces, primarily observed as small pits. These surface changes were not observed after exposure in water, with the exception of PBO, in which the surface morphological changes induced by water and bleach solution were roughly the same.

Chemical analysis of bleach-exposed fibers via FTIR revealed significant chemical changes initiated by the strong oxidizers in bleach. Hydrolytic degradation was observed for the aramids and PBO, and evidence for oxidative degradation was observed for UHMWPE. Each of these damage modes can be correlated to the observed changes in fiber tensile properties.

The results of this limited study infer that chlorine bleach exposure over a period of time could be potentially damaging to soft body armor constructed from commercial aramid, UHMWPE, and PBO fibers, and should be avoided in the routine care and

cleaning of armor. Although exposure to aqueous-based cleaning and artificial perspiration solutions did not cause additional damage to ballistic fibers beyond that of water alone, it should still be noted that for aramid and PBO, water does degrade fiber mechanical properties. Therefore, it is recommended that the use of water and/or any aqueous-based products should be avoided or used minimally the daily use and care of soft body armor.

Acknowledgments

The authors thank NIST's Office of Law Enforcement Standards (OLES) and the National Institute of Justice (NIJ) under Agreement Number 2003IJR029 for their support of this research.

Table 1: Summary of ballistic fiber tensile properties (supplied by manufacturer)

	Density (g/cc)	Denier (g/9000 m)	Tensile Strength (GPa)	Elongation at Break (%)	Modulus (GPa)
Aramid Yarn	1.44	1500	2.8	3.7	70
PBO Yarn	1.54	498	5.8	3.5	180
UHMWPE Yarn	0.97	1350	3.6	---	115 - 120

Table 2: Chemical composition of artificial perspiration solutions compared to human perspiration.

COMPONENTS	Human Perspiration [7, 8]	ISO 3160-2 [9]	EN 1811 [10]
NaCl	(5.84 – 8.65) g/L	20 g/L	5 g/L
KCl	(0.067 – 1.012) g/L		
NH_4Cl		17.5 g/L	
Urea	(0.768 – 3.420) g/L	5 g/L	1 g/L
Acetic Acid		2.5 g/L	1 g/L
Lactic Acid	(0.60 – 3.60) g/L	15 g/L	
pH	4.0 – 6.8	pH adjusted to 4.7 with NaOH	pH adjusted to 6.6 with NH_4OH

Table 3: pH values for artificial perspiration, cleaning chemical solutions, and water, before and after 59 immersion cycles.

	Initial pH	Final pH (after 50 cycles)
Water	7.43	7.34
Artificial Perspiration	4.63	4.67
Bleach	5.83	5.74
Odor neutralizer	8.80	5.90
Detergent	8.64	8.5

Table 4: Percentage changes in tensile properties of ballistic fibers following artificial perspiration and cleaning chemical exposure, relative to baseline properties.

	Dry			Water			Artificial Perspiration			Odor Neutralizer			Bleach			Detergent		
	σ_{max}	ε_{max}	E_{young}	σ_{max}	ε_{max}	E_{young}	σ_{max}	ε_{max}	E_{young}	σ_{max}	ε_{max}	E_{young}	σ_{max}	ε_{max}	E_{young}	σ_{max}	ε_{max}	E_{young}
Aramid Yarn	-10.18	-27.15	5.59	-13.67	-22.96	2.01	-24.07	-26.26	-4.60	-21.70	-22.13	-6.36	-60.12	-49.48	-28.93	-15.66	-24.68	3.58
Scoured Aramid Fabric	-19.01	-8.71	-5.33	-33.18	-32.84	-1.22	-9.61	-20.25	3.75	-26.53	-20.30	-13.49	-49.54	-33.57	-23.79	-29.23	-23.06	-4.42
WRT Aramid Fabric	-11.71	-10.53	-4.99	-23.15	-24.35	-0.22	-11.06	-14.44	3.37	-14.40	-21.18	-5.43	-49.07	-35.53	-14.70	-17.80	-23.32	15.95
PBO	-21.22	-19.39	-0.14	-39.07	-35.99	0.84	-36.20	-27.62	-7.81	-34.09	-37.45	10.49	-45.68	-40.15	-10.10	-47.40	-48.69	2.45
UMHWPE	10.50	7.74	2.32	-0.56	1.56	3.38	-9.19	8.22	0.94	0.49	1.01	2.47	-18.81	-1.39	-3.90	-6.34	-2.79	1.01

statistically significant

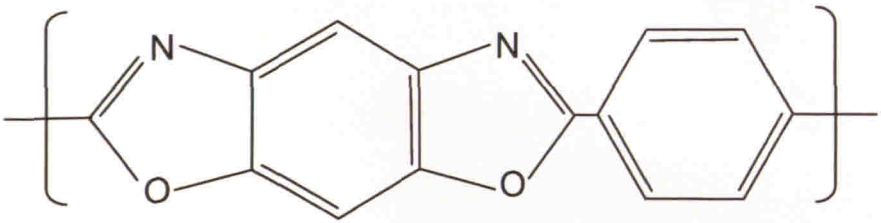

Figure 1: Chemical structure of poly(p-phenylenebenzobisoxazole)

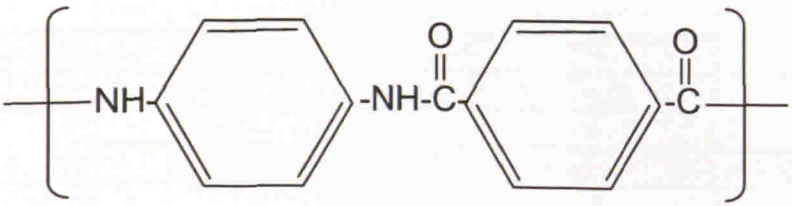

Figure 2: Chemical structure of poly(p-phenylene terephthalamide)

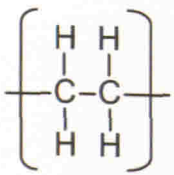

Figure 3: Chemical structure of UHMWPE

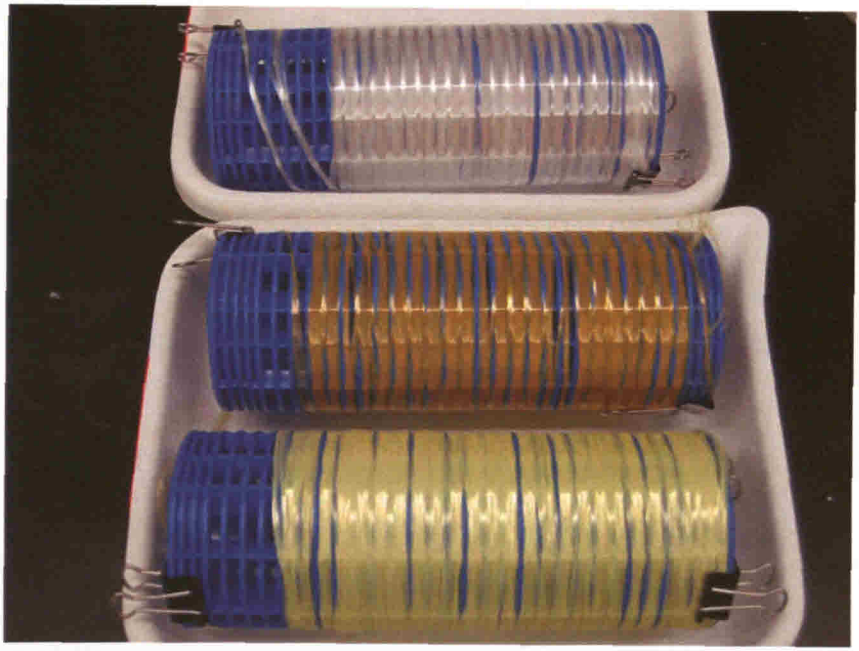

Figure 4: Fibers wound on dye tubes

Figure 5: Samples in oven at 40 °C.

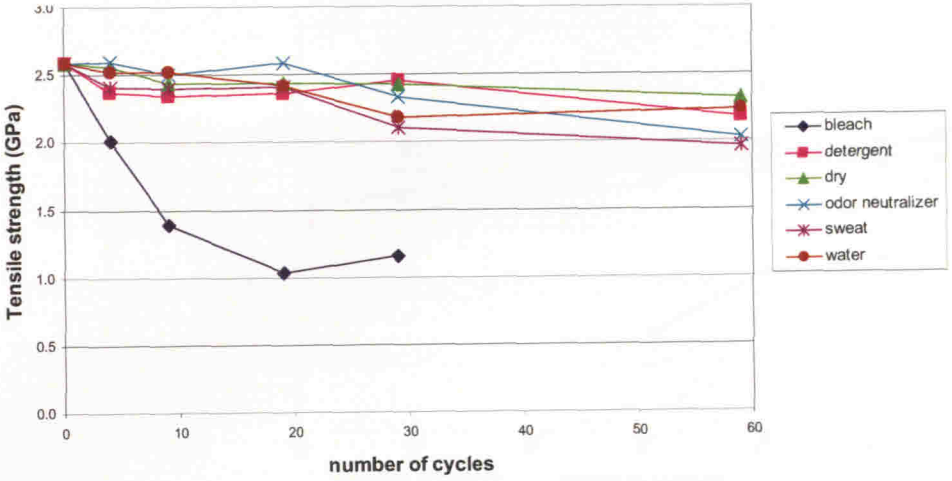

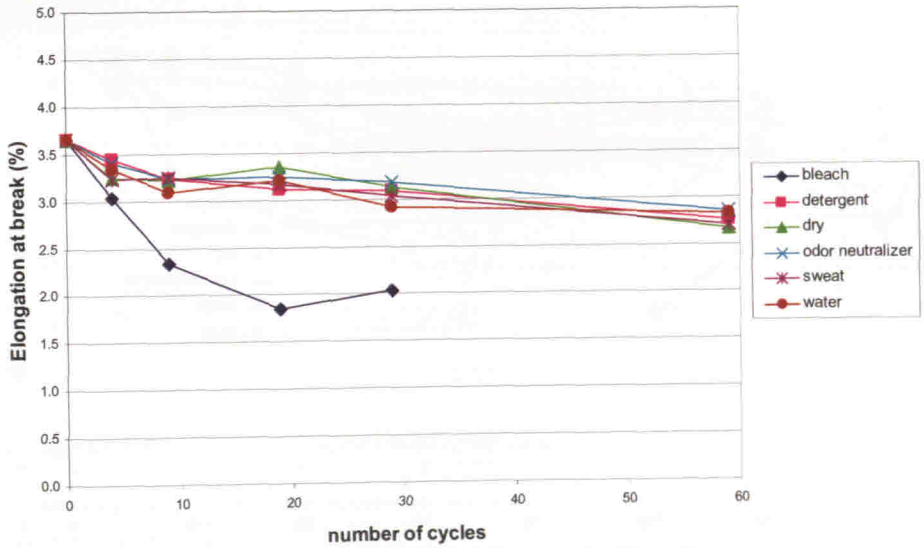

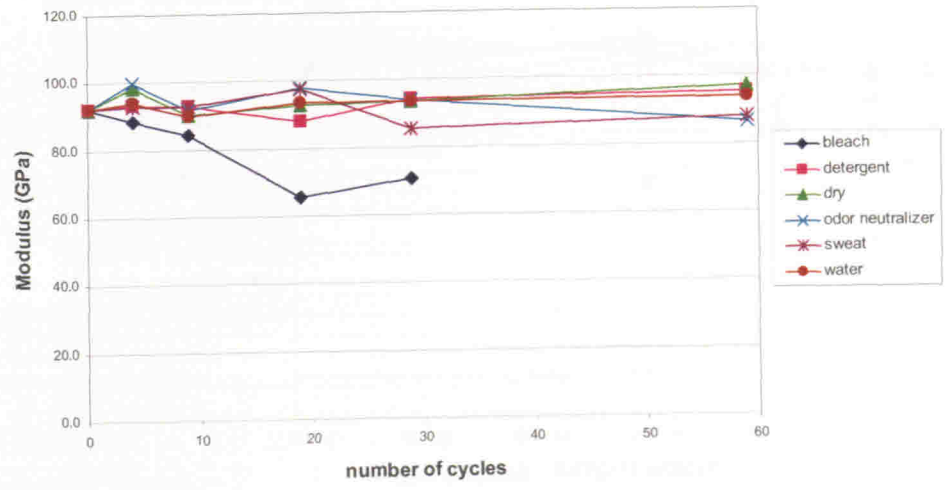

Figure 6: Evolution of the tensile strength, elongation at break, and modulus of aramid yarn as a function of artificial perspiration and cleaning chemical immersion. Standard uncertainty of these measurements is typically ± 5 %.

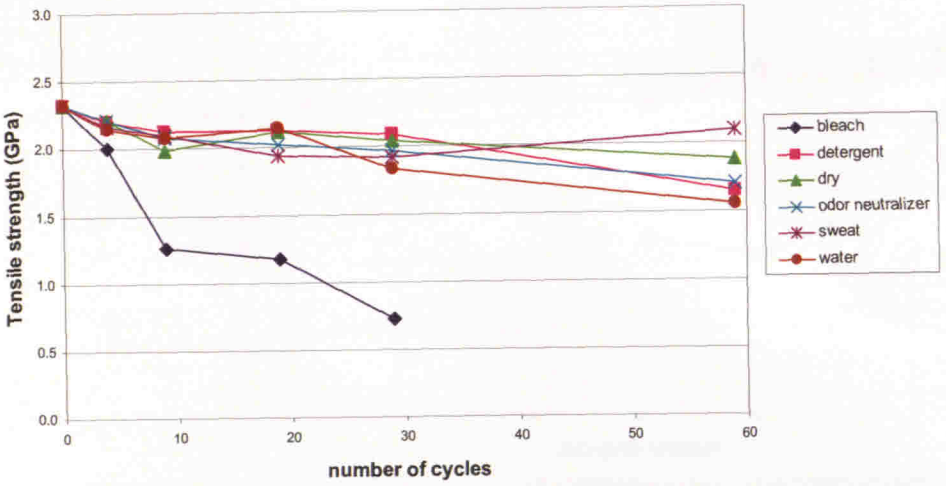

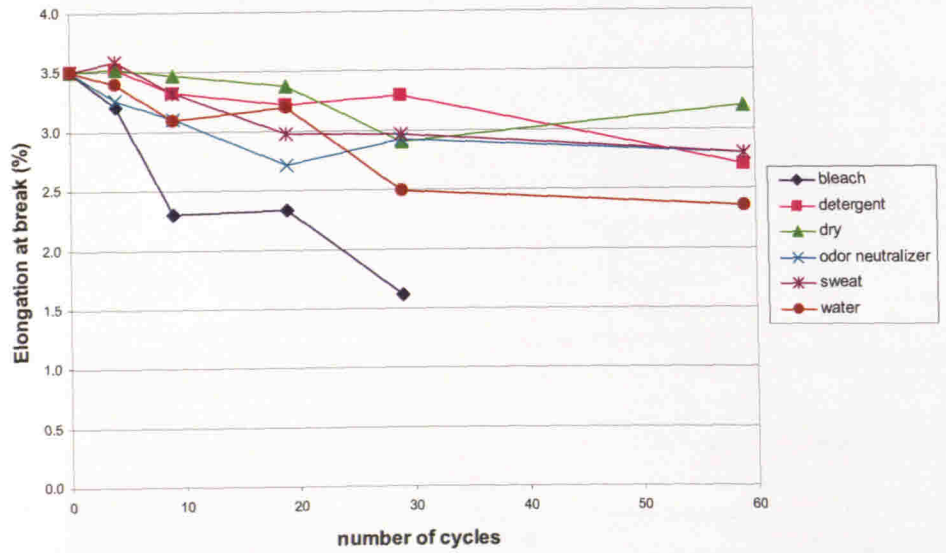

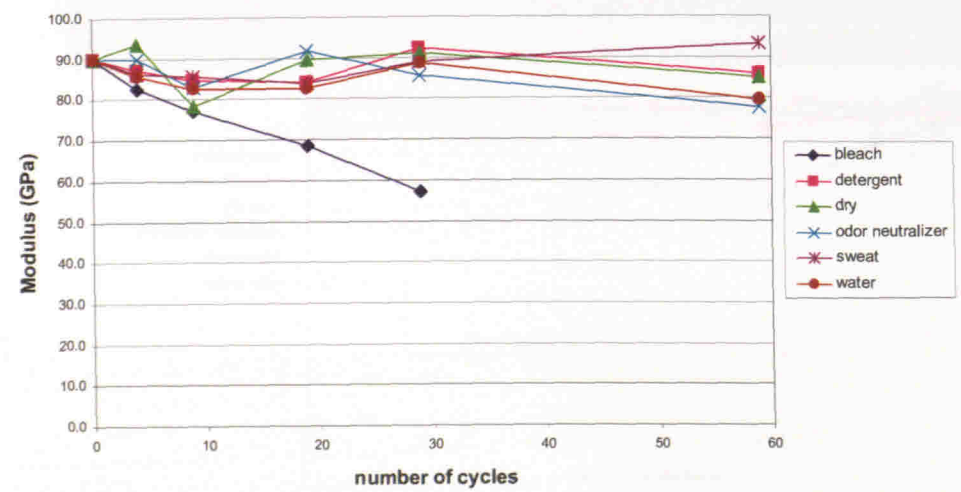

Figure 7: Evolution of the tensile strength, elongation at break, and modulus of yarns extracted from scoured aramid fabric as a function of artificial perspiration and cleaning chemical immersion. Standard uncertainty of these measurements is typically ± 5 %.

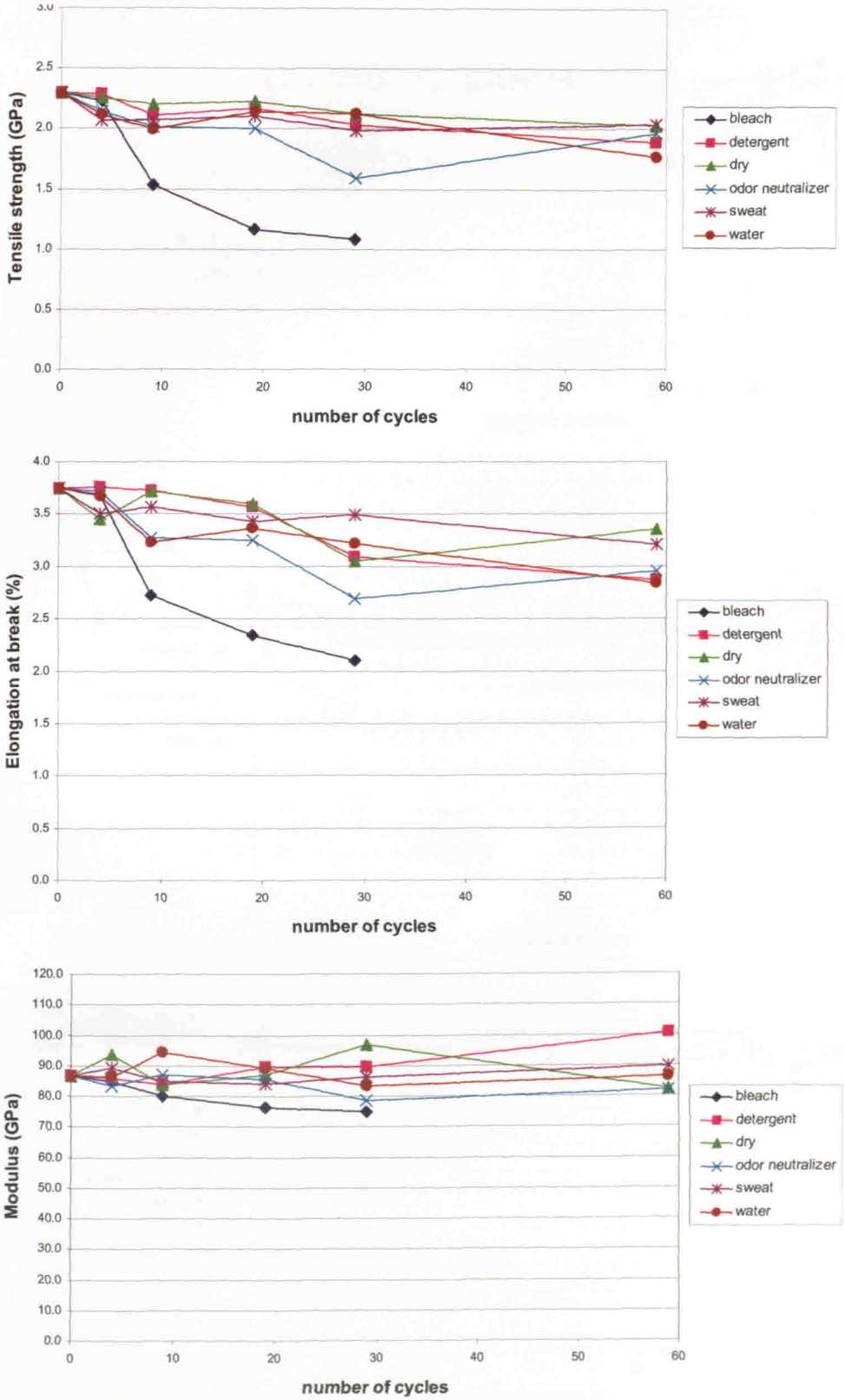

Figure 8: Evolution of the tensile strength, elongation at break, and modulus of yarns extracted from WRT aramid fabric as a function of artificial perspiration and cleaning chemical immersion. Standard uncertainty of these measurements is typically ± 5 %.

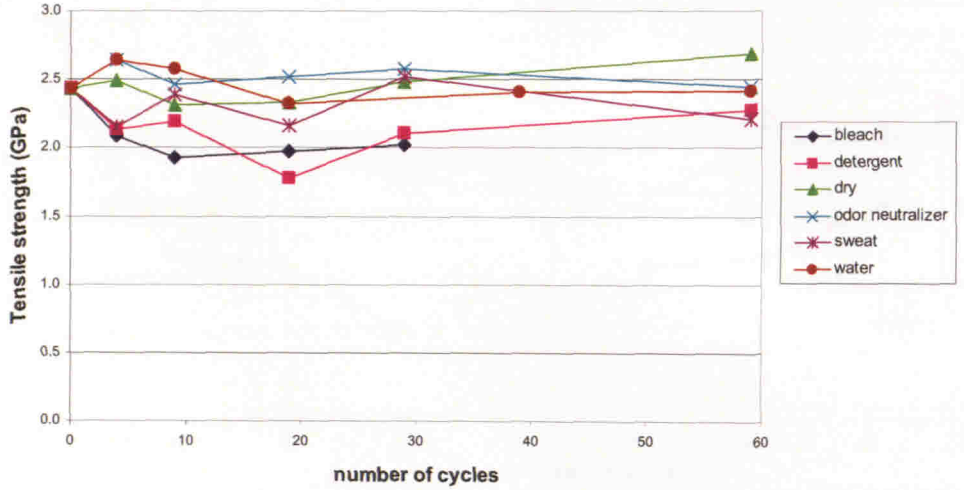

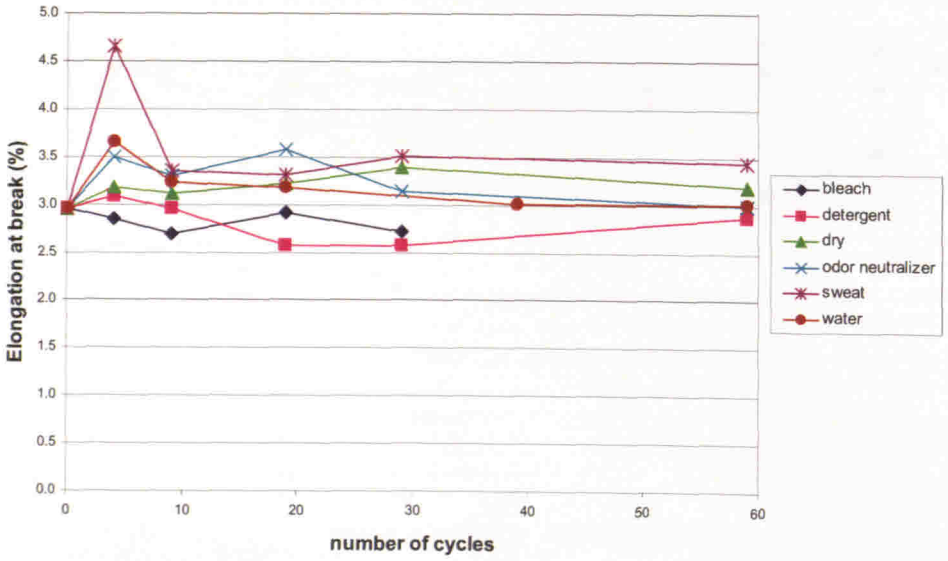

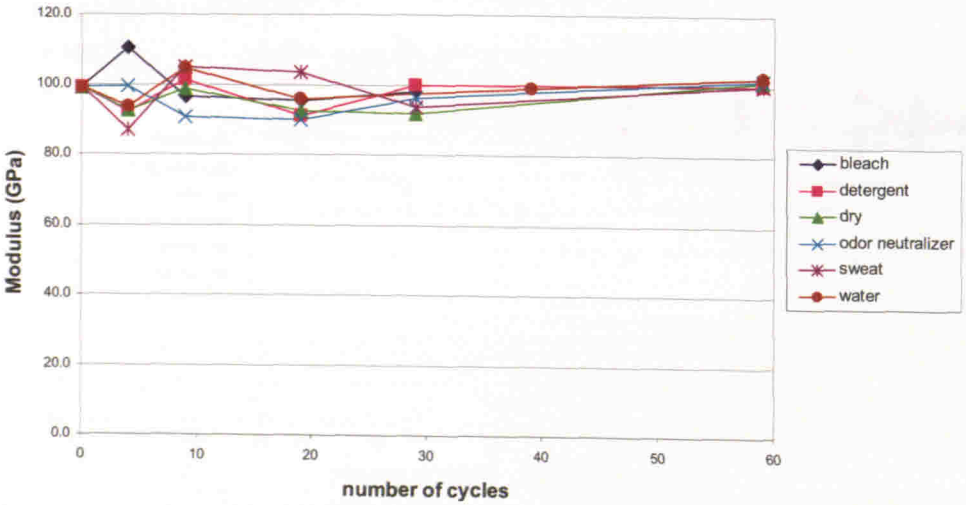

Figure 9: Evolution of the tensile strength, elongation at break, and modulus of UHMWPE yarns as a function of artificial perspiration and cleaning chemical immersion. Standard uncertainty of these measurements is typically ± 5 %.

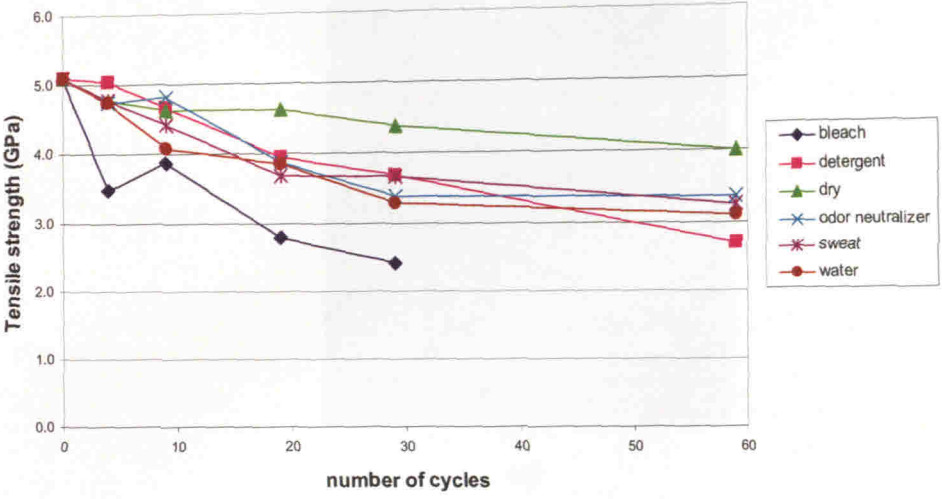

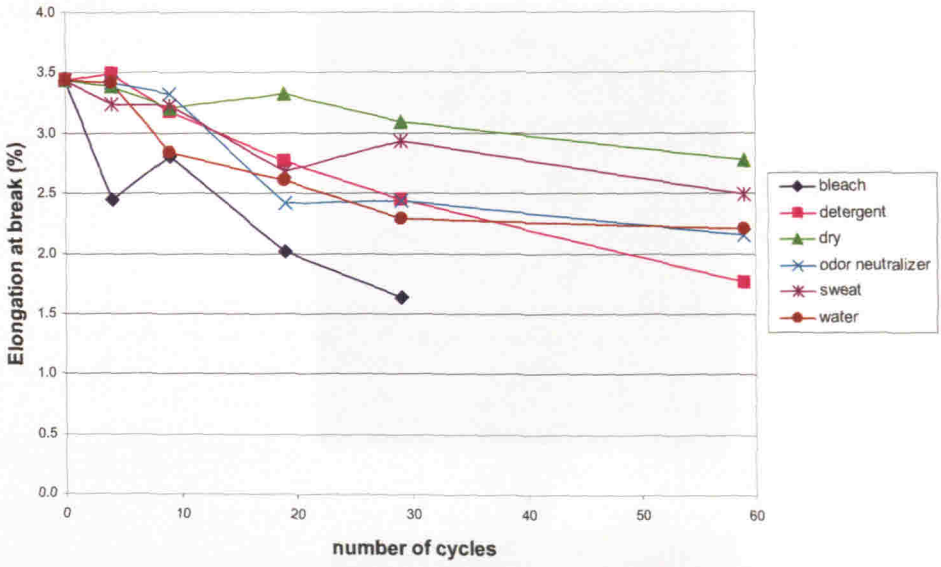

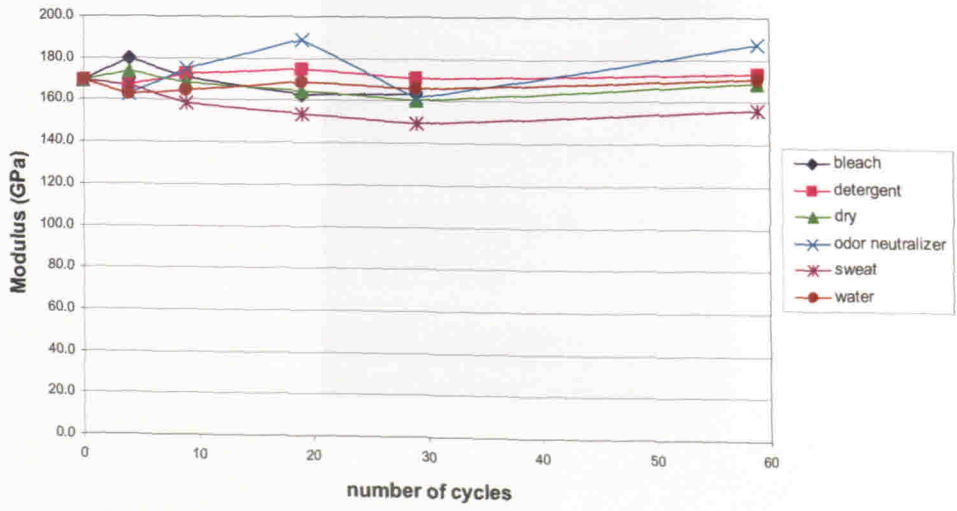

Figure 10: Evolution of the tensile strength, elongation at break, and modulus of PBO yarns as a function of artificial perspiration and cleaning chemical immersion. Standard uncertainty of these measurements is typically ± 5 %.

(a)

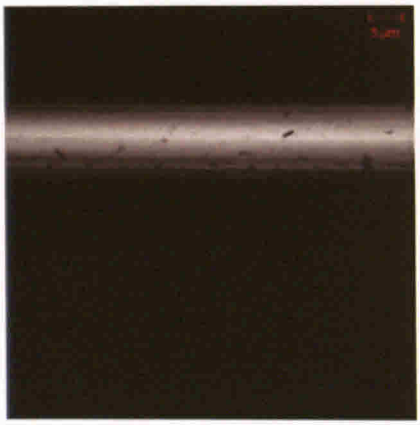

(b)

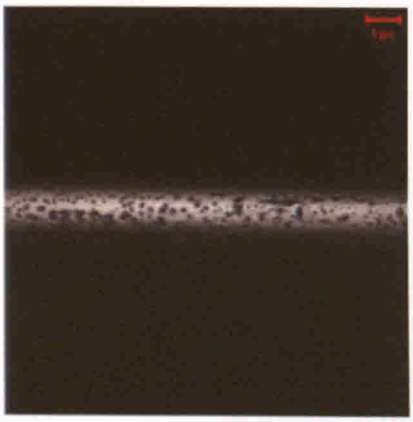

(c)

Figure 11: Representative confocal microscope images of aramid fibers (a) before exposure, (b) after 29 cycles of water exposure, and (c) after 29 cycles of bleach solution exposure.

(a)

(b)

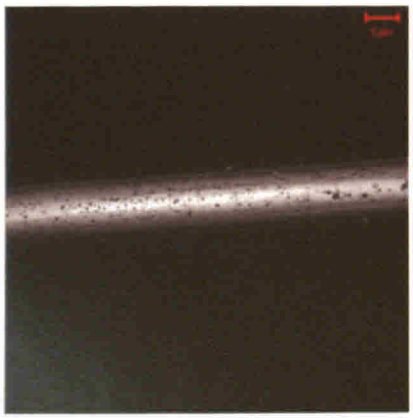

(c)

Figure 12: Representative confocal microscope images of fibers extracted from scoured aramid fabric (a) before exposure, (b) after 29 cycles of water exposure, and (c) after 29 cycles of bleach solution exposure.

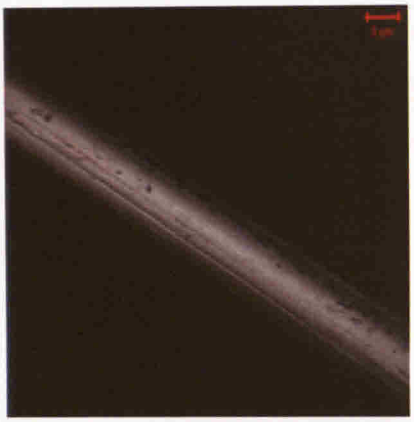

(a)

(b)

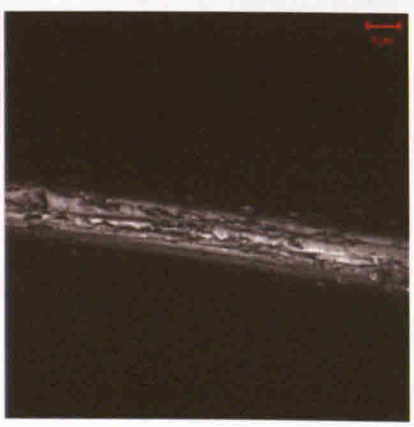

(c)

Figure 13: Representative confocal microscope images of fibers extracted from WRT aramid fabric (a) before exposure, (b) after 29 cycles of water exposure, and (c) after 29 cycles of bleach solution exposure.

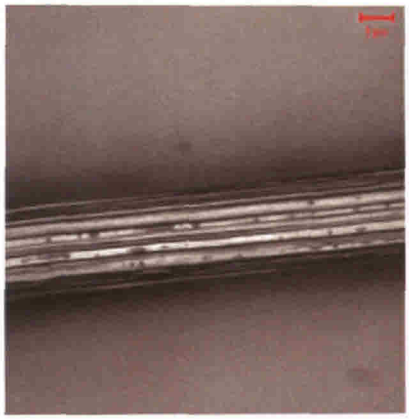

(a)

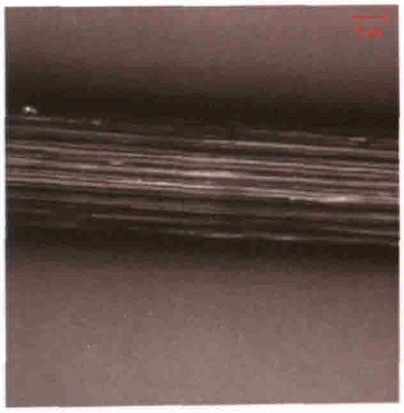

(b)

(c)

Figure 14: Representative confocal microscope images of UHMWPE fibers (a) before exposure, (b) after 29 cycles of water exposure, and (c) after 29 cycles of bleach solution exposure.

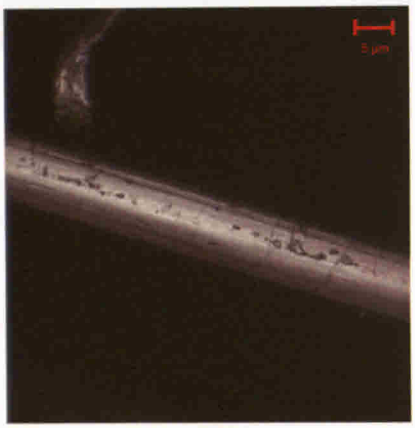

(a)

(b)

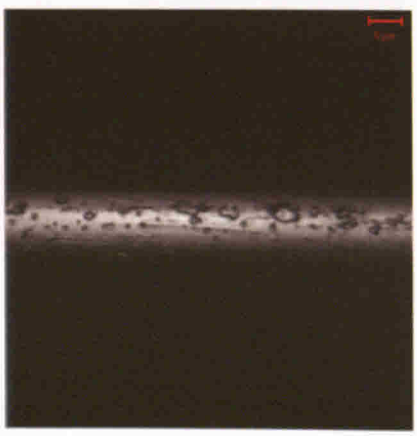

(c)

Figure 15: Representative confocal microscope images of PBO fibers (a) before exposure, (b) after 29 cycles of water exposure, and (c) after 29 cycles of bleach solution exposure.

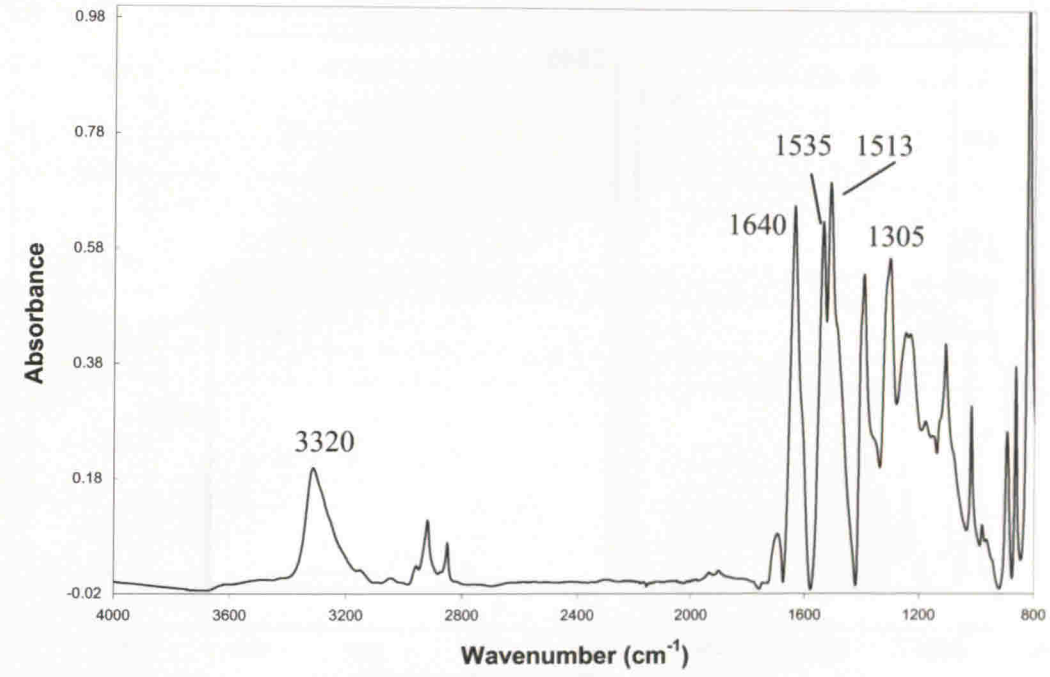

(a)

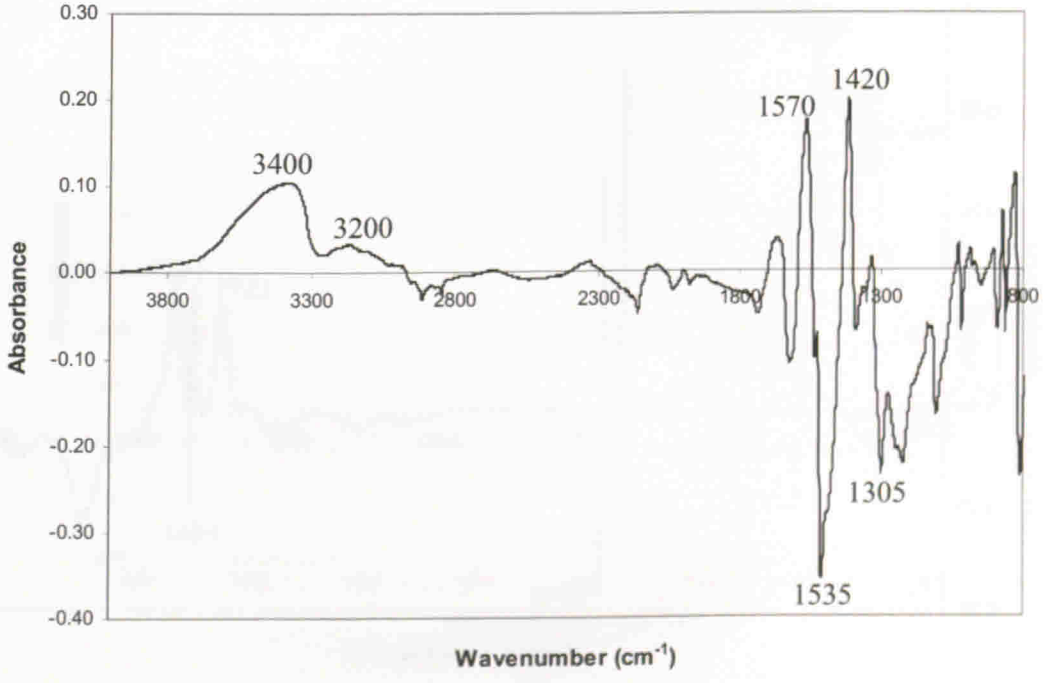

(b)

Figure 16: (a) FTIR spectrum of unexposed aramid yarns, and (b) Difference spectrum of aramid yarns following 29 cycles of bleach solution exposure, referenced to spectrum of unexposed yarn.

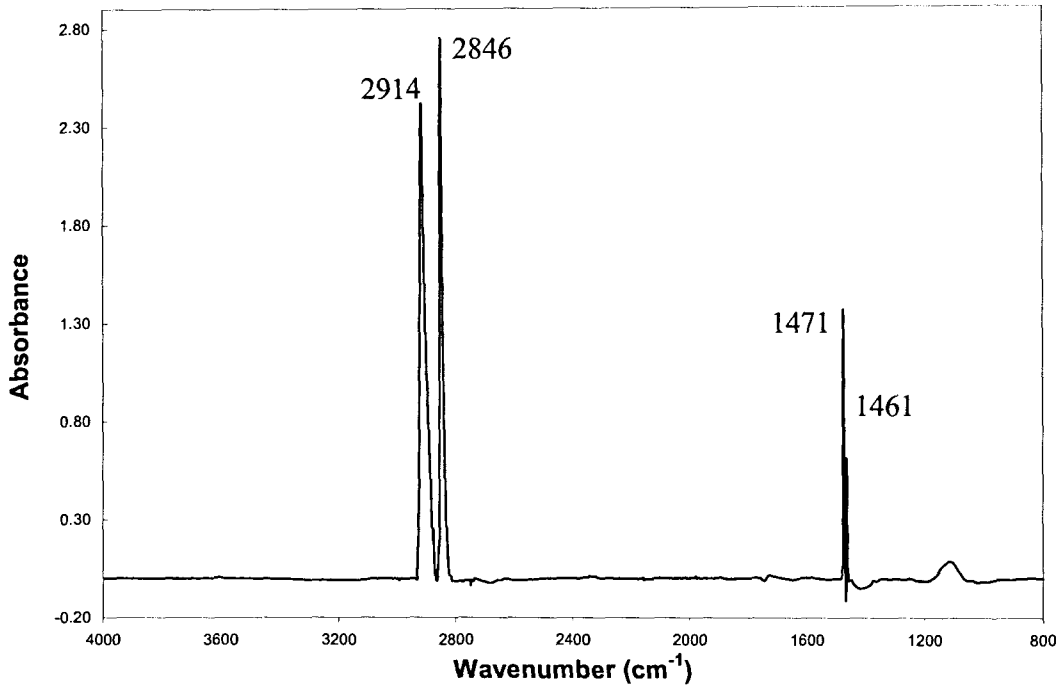

(a)

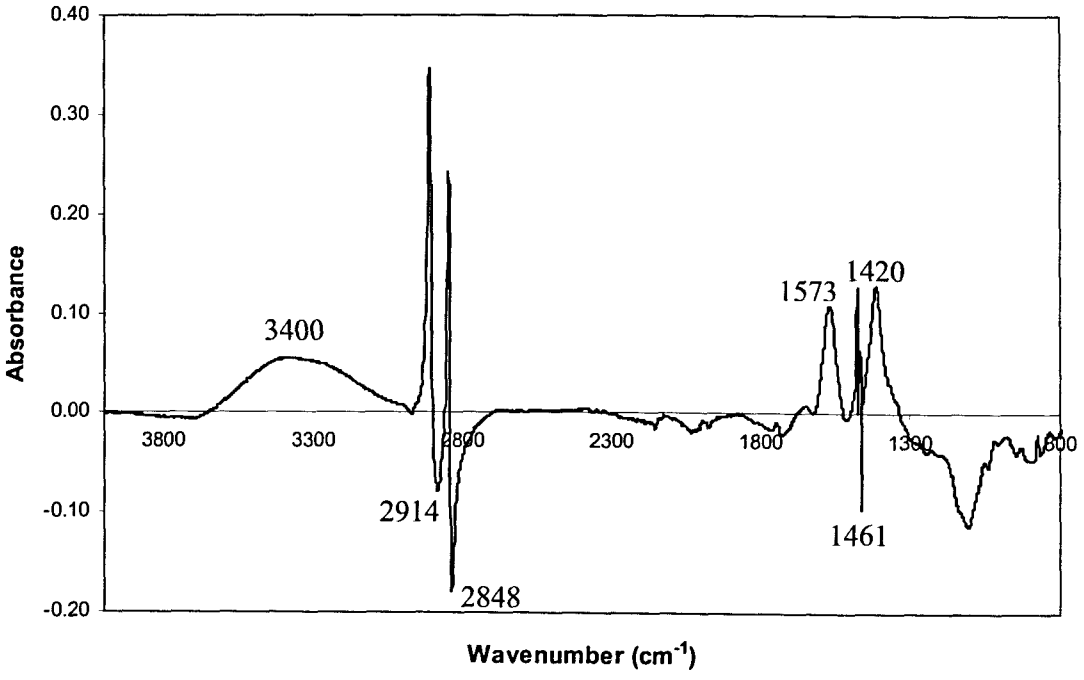

(b)

Figure 17: (a) Spectrum of unexposed UHMWPE yarns and (b) Difference spectrum of UHMWPE yarns following 29 cycles of bleach solution exposure, referenced to spectrum of unexposed yarn.

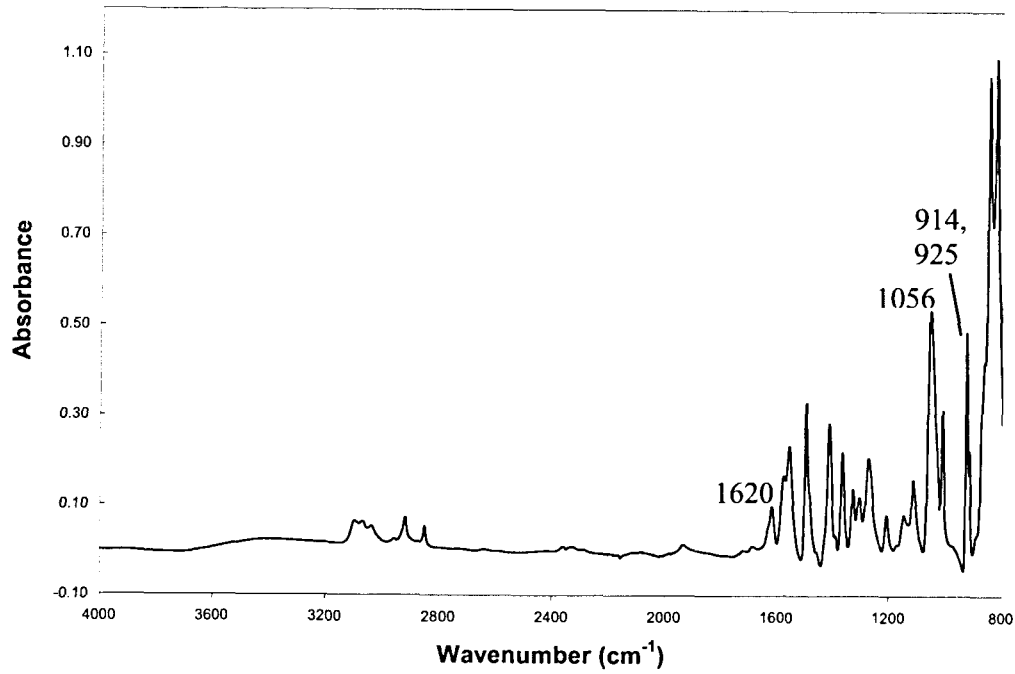

(a)

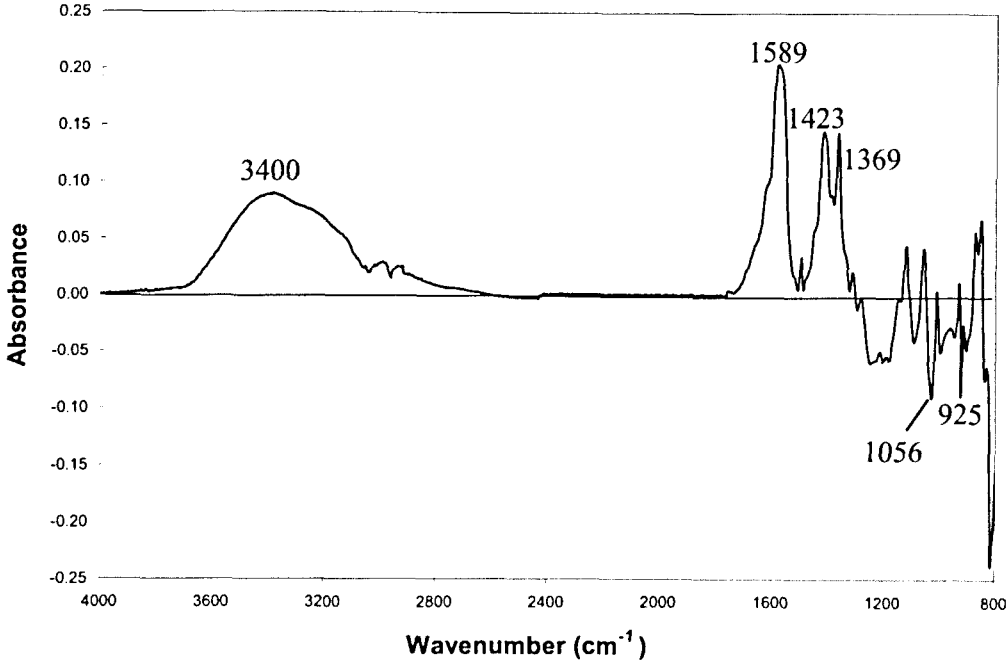

(b)

Figure 18: (a) Spectrum of unexposed PBO yarns, and (b) Difference spectrum of PBO yarns following 29 cycles of bleach solution exposure, referenced to spectrum of unexposed yarn.

References

[1] S. Ran, C. Burger, D. Fang, X. Zong, B. Chu, B.S. Hsiao, Y. Ohta, K. Yabuki, and P.M. Cunniff, *Macromolecules*, **35**(27), 9851-9853 (2002).

[2] X.-D. Hu, S.E. Jenkins, B.G. Min, M.B. Polk, and S. Kumar, *Macromol. Mater. Eng.*, **288**, 823-843 (2003)

[3] E. Orndoff, *NASA Technical Memorandum 104814*, September 1995

[4] J.W. Chin, A. Forster, C. Clerici, L. Sung, M. Oudina, and K. Rice , April 2006, *NISTIR 7373*, April 2006.

[5] H.H Yang, *Kevlar Aramid Fiber* (John Wiley & Sons Ltd, 1993).

[6] W. Hoogsteen, A. J. Pennings and G.T.Brinke, *Colloid. Polym Sci*, **268**, 245-255 (1990).

[7] S. Robinson and H. Robinson, *Physiol Rev.*, **34**, 202-220 (1954).

[8] G.W. Cage and R.L. Dobson, *Journal of Clinical Investigation*, **44(7)**, 1270-1276 (1965).

[9] ISO 3160-2, "Watch-cases and accessories - Gold alloy coverings Part 2: Determination of fineness, thickness, corrosion resistance and adhesion."

[10] EN1811, "Reference test method for release of nickel from products intended to come into direct and prolonged contact with the skin" (1998).

[11] B. Dickens in *Service Life Prediction Methodology and Metrologies*, J.W. Martin and D.R. Bauer, eds. (American Chemical Society, 2001).

[12] B. A. Cheeseman and T. A. Bogetti, *Composite Structure,* **61**, 161–173(2003)

[13] J.L.Devors, *Probability & Statistics for Engineering and the Sciences* (Brooks/Cole Publishing Company, 1982)

[14] R.J. Morgan, C.O. Pruneda, N. Butler, F.-M. Kong, L. Caley and R.L. Moore, *Proceedings of the 29th National SAMPE Symposium*, April 1984.

[15] Y.-H. So, S.J. Martin, K. Owen, P.B. Smith and C.L. Karas, *J. Polym. Sci., Part A: Polym. Chem.*,**37**, 2637(1999).

[16] R.M. Silverstein, G. C. Bassler, and T.C. Morrill, *Spectrometric Identification of Organic Compounds*, 4th edition (John Wiley and Sons, 1981).

[17] L. Penn and F. Larsen, *J. Appl. Polym. Sci.*, **23**, 59-73 (1979)

[18] A.L. Dos Santos Alves, L.F.C. Nascimento, and J.C. M. Suarez, *PolymerTesting*, **24**, 104-113 (2005).

[19] R. Foerch, J. Izawa, and G. Spears, *J. Adhesion Sci. Technol.*, **5**(7), 549-564 (1991).

[20] K. Tamargo-Martinez, S. Villar-Rodil, J.I. Paredes, A. Martinez-Alonso, and J.M.D. Tascon, *Chem. Mater.*, **15**, 4052 (2003).

[21] Y.J. Kim, B.R. Einsla, C.N. Tchatchoua, and J.E. McGrath, *High Performance Polymers*, **17**, 377 (2005).